Athens Journal of Technology and Engineering - Volume 12, Issue 4, December 2025 – Pages 281-292

Impact of GFRP Reinforcement Ratios on the Behavior Full-scale Concrete Bridge Deck Slabs

By Rajai Z. Al-Rousan, Khairedin M. Abdalla±, Nikos D. Lagaros° & Bara'a R. Alnemrawi•*

The purpose of the research paper in hand is to investigate the effect of axially applied and cyclic lateral loadings on the effectiveness of using carbon fiber-reinforced polymer (CFRP) material in preserving the structure's behavior as well as governing the failure's mode of the different-in-strength-of-concrete CFT circular-shaped steel columns. For this purpose, the nonlinear finite element analysis (NLFEA) method has been employed. To begin with, a CFT column model was verified using the findings of previously published research; then, the experimental model was extended to include the influence of concrete's strength in the search. Eighteen FEA CFT column samples were prepared and confined – at their ends – with different numbers of CFRP layers, representing the crucial position (with respect to the lateral loading capacity) and, also, to prevent the column samples from localized buckling outwardly. Thus, the samples would acquire more strength, greater net drifting, and higher dissipation of energy. The parameters of the experimental research were: i) the number of CFRP's layers, and ii) the level of axial load. The research aimed to numerically explore, utilizing NLFEA, the influence of the research's parameters on the CFT FEA models' behavior after the samples had been put to adequate calibration and validation as per credible experimental findings. The obtained findings indicated that when the columns were strengthened with CFRP, there was an enhancement in the cyclic behavior, represented by: more improved capacity of load, bigger horizontally oriented displacements, more displacement's ductility, more dissipated energy, and less deterioration in secant stiffness

Keywords: *concrete strength, CFT columns, CFRP, lateral loading, cyclic axial loading, NLFEA*

Introduction

It is stipulated that the steel CFT (i.e., concrete-filled tubular) columns often encounter outward local buckling, where the inward type of buckling is inhibited by concrete. When resisting moments or frames of sway, the CFT columns are exposed to axial and lateral loading which induces moments within columns; noting that the ends of columns encounter the highest level of moments. Thus, the region of the column's end is taken as a critical location that is exposed to the influence of a

*Professor, Department of Civil Engineering, Jordan University of Science & Technology, Jordan.
±Professor, Department of Civil Engineering, Jordan University of Science & Technology, Jordan.
°Professor, Department of Structural Engineering, National Technical University of Athens (NTUA), Greece.
•Department of Civil Engineering, Jordan University of Science & Technology, Jordan.

https://doi.org/10.30958/ajte.12-4-4 doi=10.30958/ajte.12-4-4

combination of lateral and axial loadings. Concerning seismic designing, the resisting-to-moment frame's column must have the ability to withstand plastic lateral deformation and enough ductility. The CFT column's behavior has been researched by a large number of credible researchers (Shen et al. 2024, Amer et al. 2023, Alnemrawi and Al-Rousan 2024a); among those was Xiao (2004) who suggested confining the end region of a CFT column with FRP, aiming at preventing the columns from outward local buckling and enhancing the columns' strength as well as ductility. Also, this technique enhances the behavior of the internal concrete, particularly in the case of having columns' ends with high stresses (Teng et al. 2012, Al-Rousan et al. 2024). Much research has been carried out to investigate the usefulness of confining the CFT columns' ends with FRP (Al-Rousan and Alnemrawi 2023, Yu et al. 2016). Some researchers investigated the effectiveness of wrapping under-monotonic-axial-compression CFT circular columns with glass-FRP material when these columns were exposed to a monotonic type of axial compression (Güneyisi and Nour 2019) and cyclic type of axial compression (Teng et al. 2013). However, only a limited number of researchers studied the wrapped-with-FRP CFT steel columns' seismic performance (Du et al. 2021); they found that the wrapped-with-FRP CFT steel columns exhibited a marvelous resistance to seismic actions, regardless of whether the columns were circular or squared.

It is worth mentioning that only a limited number of research used the NLFEA to analyze – numerically – the structures' response when subjected to a seismic load (Ren et al. 2022, Shaaban and Said 2018, Al-Rousan and Alkhawaldeh 2021). Studying the CFT columns' response – when subjected to axial and cyclic lateral loads – is a rather difficult task because a special-purpose setup and unique-capacity testing machine are required to fulfill such studies (Al-Rousan et al. 2021). Hence, it is highly valuable to have credible experimental findings related to this matter, as such findings can be of much assistance in creating and validating accurate and strong NLFEA simulations to real-life ones (Alhassan et al. 2018, Al-Rousan 2022, Al-Rousan 2020). After being properly validated, the simulated-via-NLFEA model could be enlarged for the sake of running a parametric study to investigate the influence of multiple parameters, for example: the level of applied axial loading and the quantity of wrapping layers of FRP (Abdalla et al. 2020, Al-Rousan and Sharma 2021). To attain unique and worthy findings, the research in hand employs NLFEA to simulate the response of confined-with-CFRP CFT circular-shaped and made-of-steel columns when exposed to cyclic lateral and axial loads. The FEA-simulated models were put to an adequate validation as per the findings of Yu et al. (2016) achieved from experiments run on big-scale, cantilever columns; then, the model was expanded to include the influence of concrete's strength.

Modeling Methodology

Figure 1 displays the geometric properties of the simulated model, along with the setup diagram of the experiment (Yu et al. 2016). The CFT column model had a diameter of 318 mm and a height of 1625 mm; the model was strongly fastened to a rigid RC footing that had a length of 1500 mm, a width of 1400 mm, and a thickness of 550 mm. The whole model had steel tubes with a thickness of 3 mm

and a 106, which represents the diameter-to-thickness ratio. The ends of the column samples (at 500 mm) were wrapped with CFRP jackets to obtain a complete plastic hinging and develop good ductility and toughness.

Figure 1. *The Diagram of the Experiment's Setup - Dimensions in mm (Yu et al. 2016)*

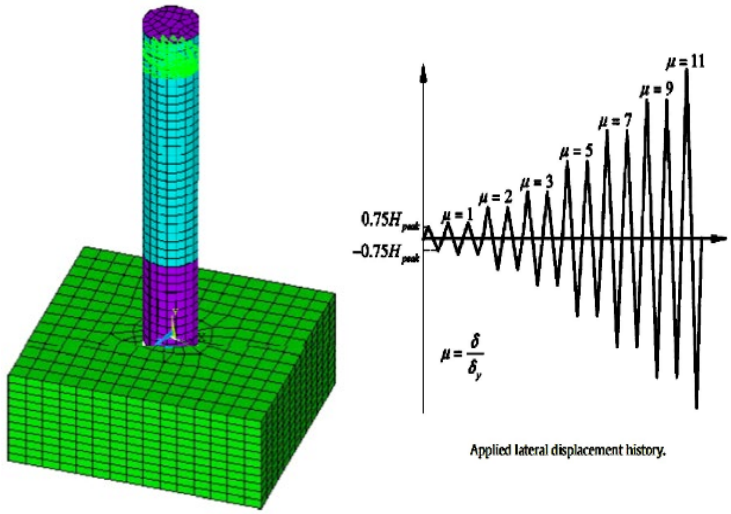

The discretization of the CFT column models was done utilizing the ANSYS (2016) along with three-dimensional isoperimetric solid elements that had eight defining nodes (Figure 1). The best-fit density of mesh was specified by carrying out a convergence study. As for the boundary conditions, the columns' lower ends were made fixed, while the upper ends could move freely. The concrete was simulated utilizing the element SOLID65, which had eight with-three-degree-freedom nodes and could move in every direction; also, this element had the capabilities of cracking, plastic deforming, and crushing in three perpendicular orientations. The Solid65 element's capability of concrete crushing was not considered upon simulating the models because it was not experimentally noticed. Hence, the models' ultimate failure and concrete's cracking depended totally on the in-tension strains. Since the stipulated concrete's Poisson ratio was between 0.15 and 0.22, the current research chose the ratio to be 0.2 (Al-Rousan et al. 2022). The criterion of concrete failure was defined by using each of the at-ultimate strengths in compression (Figure 2), the in-tension strength (Figure 2), and Young's modulus of elasticity (ACI Committee 2019). The condition of the face of cracking was defined by the coefficient of shear transfer (β_t) which was 0.2 (the universal value). To ensure that the FE model was accurate, the model of Kent and Park (1971) was utilized for the concrete's compressive stress-strain formula (Figure 1). Figure 1 shows the not-linear graph of stress vs strain that was employed for modeling concrete utilizing ANSYS, as the concrete's in-compression strength was: 40, 30, and 20 MPa, and Poisson's ratio was 0.20. Solid65 had the capability of representing one rigid substance and a maximum of three various reinforcing materials. The concrete was presumed isotropic up till the emergence of cracking and then, encountered plasticity.

Figure 2. *Concrete Stress-Strain Curve (Yu et al. 2016)*

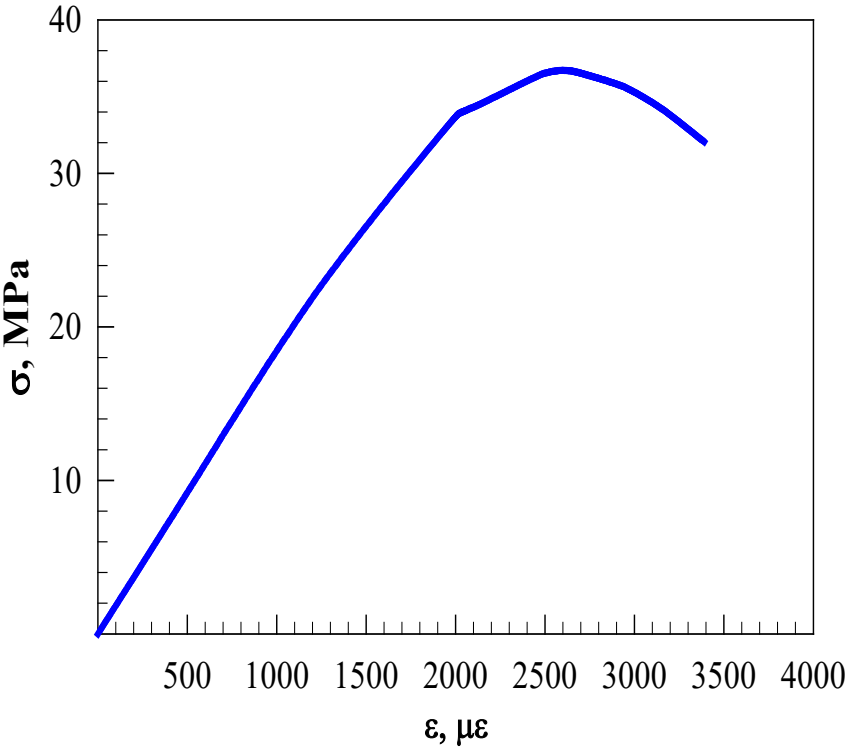

The element of SOLID45 could move in every direction, and it was utilized to simulate the steel plates and circular-shaped tubes of steel. The linear performance of elastic stress-strain was employed with a value of: Young's modulus of 203 GPa, yield's stress of 271 MPa, at-ultimate stress of 353 MPa, and Poisson's ratio of 0.30. This element (Solid45) was employed for simulating the confining CFRP, having a modulus of elasticity of 237.8 GPa and an at-ultimate strain of 0.85%, making the thickness equal to 0.34 mm (Yu et al. 2016). The concrete-tube and CFRP-tube bonds were assumingly perfect; that was achieved by joining the coinciding nodes together. The column was subjected to axial load at the initial step of loading; then, a horizontal load was incrementally exerted, as displacement-controlled, in order to determine the reducing portion of the graph of load vs displacement.

Figure 3. *Validation of the NLFEA Results*

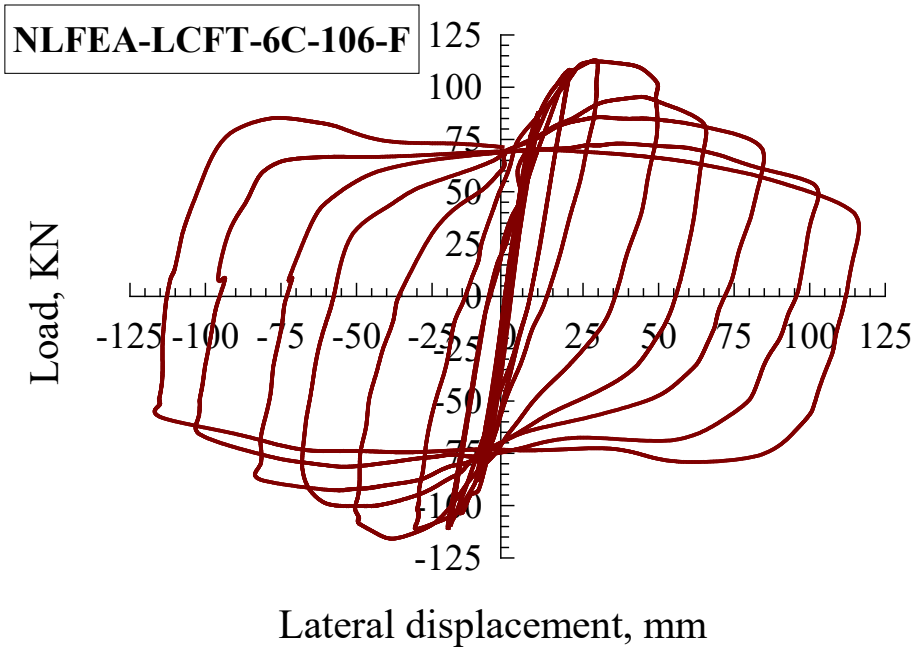

(a) NLFEA results

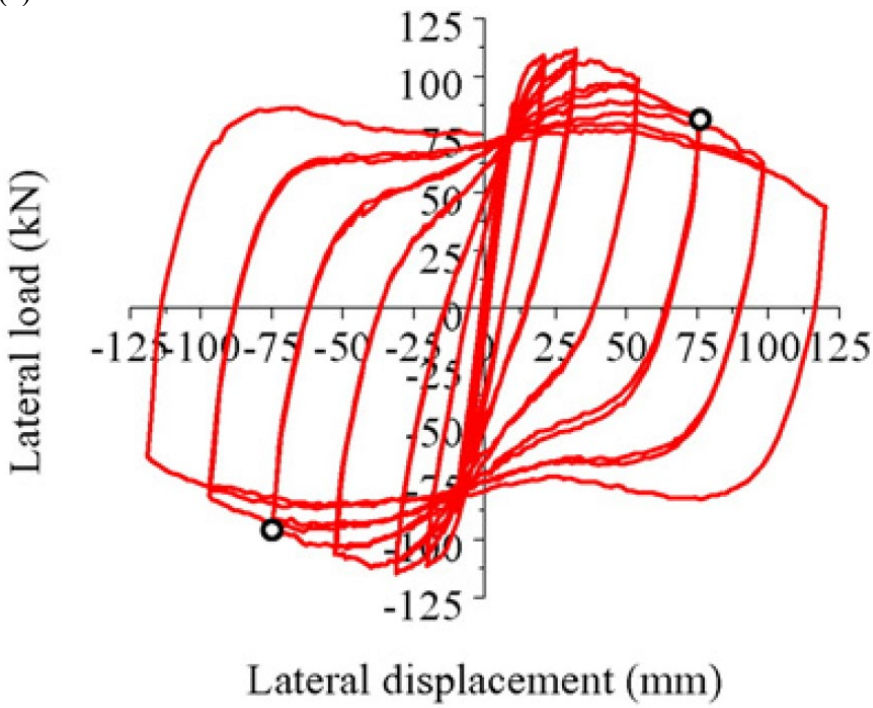

(b) Results from Yu et al. (2016)

Table 1. *NLFEA Results for Simulated CFT*

Specimen Name	Concrete Strength, MPa	CFRP Number of layers	Horizontal net drift, mm	Horizontal load, kN
CFT40C5	40	5	116.8	114.8
CFT40C6		6	122.9	120.3
CFT40C7		7	132.7	128.8
CFT40C8		8	139.8	135.5
CFT40C9		9	145.1	139.5
CFT40C10		10	148.9	141.9
CFT30C5	30	5	90.5	89.0
CFT30C6		6	94.4	92.3
CFT30C7		7	101.0	98.1
CFT30C8		8	105.4	102.2
CFT30C9		9	108.5	104.2
CFT30C10		10	110.3	105.0
CFT20C5	20	5	58.9	88.8
CFT20C6		6	62.0	96.6
CFT20C7		7	67.0	104.0
CFT20C8		8	70.5	109.9
CFT20C9		9	73.2	113.1
CFT20C10		10	75.0	116.2

To make sure that the solution was stable and prevent it from diverging, many load steps were exerted increasingly. In addition, the equilibrium iterative method of Newton-Raphson was adopted to attain a non-linear solution with 0.001 tolerance. Calibrating the FE model was made by utilizing a suitable size of mesh and an adequate load rate, in addition to taking into consideration the nonlinearities of the used materials (Al-Rousan and Alnemrawi 2024, Alnemrawi and Al-Rousan 2024b). Figure 3 indicates that the FE model's load-drift hysteresis results agreed, to a good extent, with the ones obtained experimentally by Yu et al. (2016) regarding the specimen of CFT columns wrapped with six CFRP, named LCFT-6C-106-F. Also, it was noticed that there was a remarkable agreement between the two models regarding the shapes of deformation and failure modes (Figure 3).

Nlfea Results and Discussion

Horizontal Load versus Displacement Hysteretic Response

Table 1 shows the NLFEA results for all simulated CFTs. Figure 4 displays the CFT column's prototypical hysteretic loops of the horizontal load vs displacements demonstrating the role of the CFRP layers in improving the performance of the columns, as these layers increase the lateral load capacity, the net drift capacity, and dissipated energy. Further, the reinforced-with-layers-of-CFRP CFT columns' loops of horizontal load vs displacement have indicated that the columns' behavior significantly improved, regarding displacement in the horizontal direction, and load; that is because strengthening the columns with wraps of CFRP avails the columns

with a mechanism of confinement from the external side after the CFT tube of steel has buckled.

Figure 4. *Prototypical CFT Columns' Load vs Net Drift Hysteresis Response*

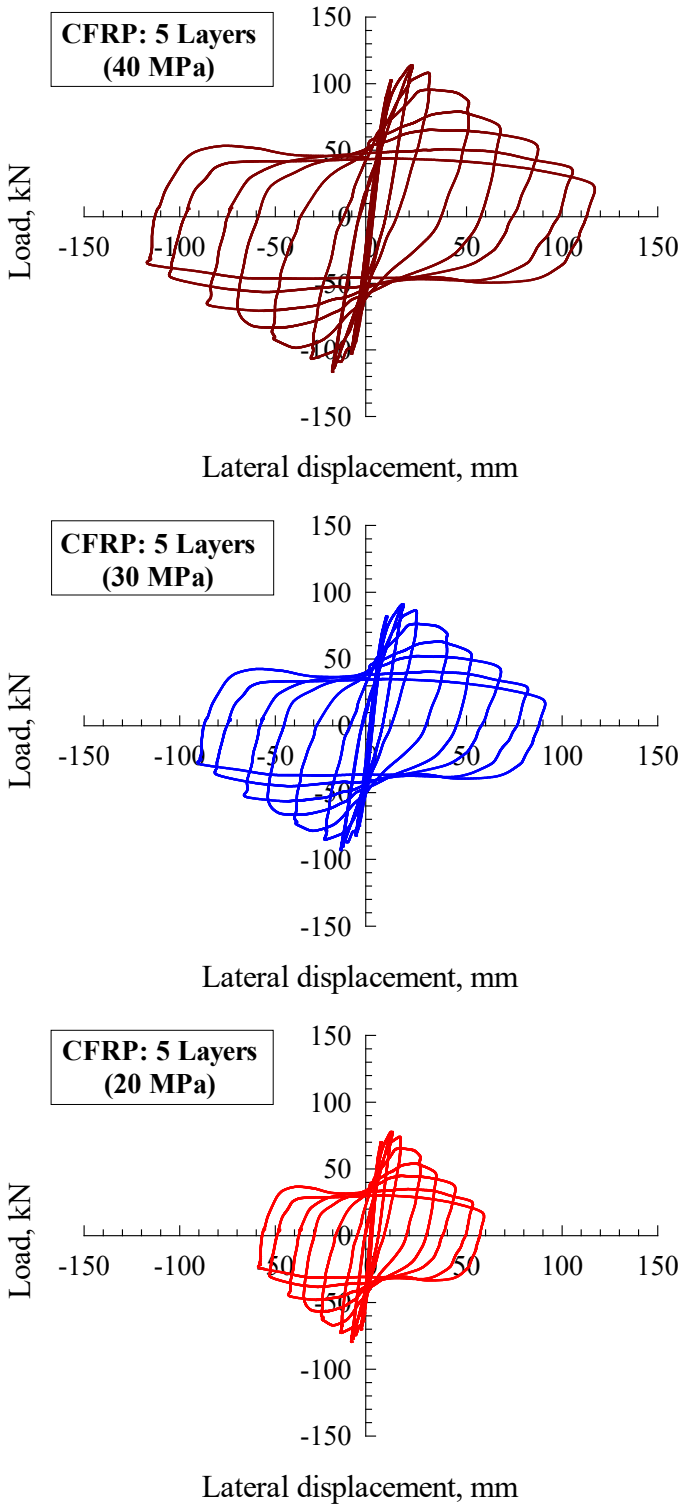

Ultimate Load and Drift Capacities

Referring to the outcomes depicted in Table 1, the following have been observed: 1) there was a disproportionate enhancement in the lateral net-drift when the column's axial load was raised, whereas the enhancement in the capacity of the lateral load was less; 2) when raising the layers of CFRP, at a given level of axial-type load, the capacities of lateral load and net-drift improved, but not in the same rate; 3) wrapping the column with 1-4 layers of CFRP have availed insignificant improvement to the behavior of columns; and 4) using 8, 9, and 10 layers of CFRP had the same influence on the column's performance. These findings evidently indicated that reinforcing CFT columns with a maximum of seven layers of CFRP considerably improved the columns' capacity of lateral load, while using eight layers improved the columns' net drift. Whereas, at 20 MPa of concrete's strength, reinforcing CFT columns of steel with up to nine layers of CFRP effectively improved the columns' capacity of lateral load, whereas the wraps of CFRP did not affect the net drift.

Lateral Displacement Versus Steel's Strain Behavior

It must be brought to attention that it is possible to investigate the behavior of the CFT columns by examining the strain levels at the end region of the steel tube. Figure 5 displays the prototypical steel tube's levels of strain against the displacement. It is noted that the strain level in the CFT column's tube of steel, at 0 level of sulfate, indicated that there was a yielding before exposing the columns to axial load, as illustrated in Figure 5. Raising the layers of CFRP, up to eight, resulted in a proportional increase in the strain levels of the tube of steel, whereas using 9 and 10 layers had a minor impact. This finding has evidently shown that wrapping the CFT columns with eight layers of CFRP was the best configuration to get the best performance.

Figure 5. *Prototypical Strains of Steel CFT Columns*

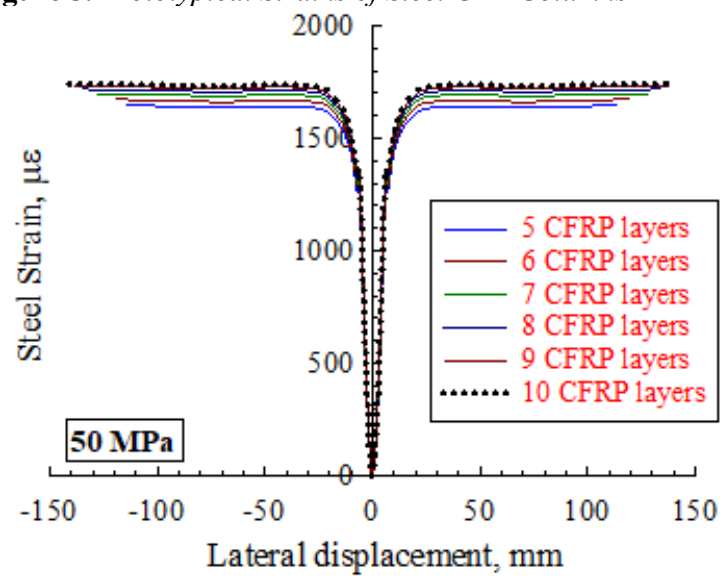

Lateral Displacement Versus CFRP Strain Behavior

Figure 6 shows the graph that displays the relation of the reinforced-with-CFRP CFT columns' horizontal displacements with the CFRP's strain. The response curve consists of two parts, as follows: the first part begins at 0 mm of horizontally directed displacement and continues up to 10 mm, whereas the second part begins at 10 mm of displacement and continues up to failure. Figure 6 indicated that the CFRP's strain swiftly rose when the horizontal displacement was slightly raised, whereas a rapid rise in horizontal displacement resulted in a little rise in the CFRP's strain. Further, it was found that utilizing up to five layers of CFRP was not sufficient to improve the CFRP's strain.

Figure 6. *Typical CFRP Strain CFT Column*

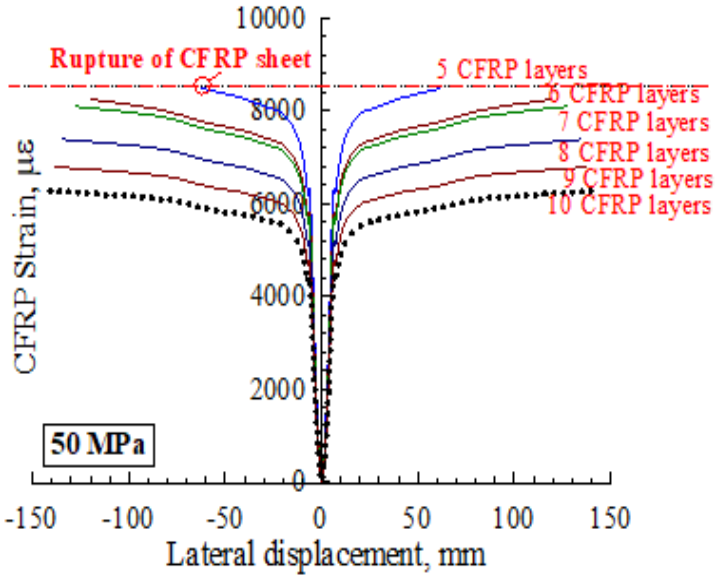

Figure 7. *Typical Stiffness Degradation*

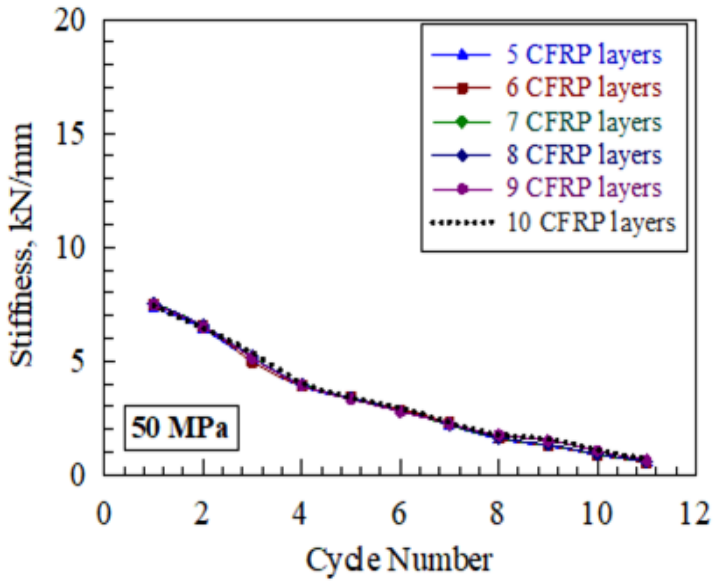

Degradation in Stiffness

The values of stiffness, at every single cycle, have been determined to plot the relation between the CFT columns' degradation in stiffness and the number of cycles, as illustrated in Figure 7. Referring to the curve of stiffness degradation vs number of cycles, Figure 7 showed that the slope (regarding the CFRP-strengthened CFT column not subjected to axial load) was greatly sharp; however, it was less sharp when the exerted axial load was raised. That was because the rise in the level of axial load availed a high level of confinement to the column-footing area.

Conclusion

Reinforcing CFT columns with wraps of CFRP enhanced the columns' lateral behavior, to a big extent. Reinforcing the FE-simulated CFT column with 5-10 CFRP wraps enhanced their lateral load and capacities of net drift - in consequence – improved the performance's factor and dissipation of energy. Several factors were found to govern the extent of improvement in CFT columns' performance, those were: properties of the column, strength of concrete, and number of CFRP layers; however, the influence of these factors was disproportionate. This is an indicator that in order to obtain significant results regarding reinforcing steel CFT columns, the simulated-through-NLFEA column model should be adequately and accurately devised. The research in hand found that confining CFT columns with eight layers of CFRP gave the best results while using 9 and 10 layers had no considerable effect.

Acknowledgments

Part of this work has been supported by the ADDOPTML – Additively Manufactured Optimized Structures by Means of Machine Learning" financed by the European Union under Horizon 2020 through the Research Funding Program: Marie Sklodowska-Curie Research and Innovation Staff Exchanges (RISE) (Project Number 101007595). Their support is highly acknowledged. The authors would like also to thank Jordan University of Science and Technology for its support.

References

Abdalla KM, Al-Rousan R, Alhassan MA, Lagaros ND (2020) Finite-element modelling of concrete-filled steel tube columns wrapped with CFRP. *Proceedings of the Institution of Civil Engineers-Structures and Buildings* 173(11): 844–857.

ACI Committee (2019) *Building code requirements for Reinforced Concrete and Commentary*. Farmington Hills, MI, USA: American Concrete Institute.

Al-Rousan RZ (2020) Behavior of Circular Reinforced Concrete Columns Confined with CFRP Composites. *Procedia Manufacturing* 44: 623–630.

Al-Rousan RZ (2022) Cyclic behavior of alkali-silica reaction-damaged reinforced concrete beam-column joints strengthened with FRP composites. *Case Studies in Construction Materials* 16(Jun): e00869.

Al-Rousan RZ, Alkhawaldeh A (2021) Behavior of heated damaged reinforced concrete beam-column joints strengthened with FRP. *Case Studies in Construction Materials* 15: e00584.

Al-Rousan RZ, Alnemrawi BR (2023) Cyclic Behavior of CFRP Confined Circular CFST Damaged by Alkali-Silica Reaction. *International Journal of Civil Engineering* 21(7): 1159–1180.

Al-Rousan RZ, Alnemrawi BR (2024) Slab slenderness effect on the punching shear failure of heat-damaged reinforced concrete flat slabs with different opening configurations and flexural reinforcement areas. *Steel and Composite Structures* 52(6): 627–645.

Al-Rousan RZ, Sharma A (2021) Integration of FRP sheet as internal reinforcement in reinforced concrete beam-column joints exposed to sulfate damaged. *Structures* 31: 891–908.

Al-Rousan RZ, Alhassan MA, Al-omary RJ (2021) Response of interior beam-column connections integrated with various schemes of CFRP composites. *Case Studies in Construction Materials* 14: e00488.

Al-Rousan RZ, Nusier O, Abdalla K, Alhassan M, Lagaros ND (2022) NLFEA of Sulfate-Damaged Circular CFT Steel Columns Confined with CFRP Composites and Subjected to Axial and Cyclic Lateral Loads. *Buildings* 12(3): 296.

Al-Rousan RZ, Alnemrawi BR, Sawalha HM (2024) The ultimate capacity of geopolymer recycled aggregate concrete filled steel tubular columns: Numerical and theoretical study. *Journal of Building Engineering* 96: 110365.

Alhassan M, Al-Rousan RZ, Amaireh LK, Barfed MH (2018) Nonlinear Finite Element Analysis of B-C Connections: Influence of the Column Axial Load, Jacket Thickness, and Fiber Dosage. *Structures* 16: 50–62.

Alnemrawi BR, Al-Rousan R (2024a) The Detailed Axial Compression Behavior of CFST Columns Infilled by Lightweight Concrete. *Buildings* 14(9): 2844.

Alnemrawi BR, Al-Rousan RZ (2024b) Numerical and analytical study on the punching shear capacity prediction for eccentrically loaded flat slabs with openings. *Results in Engineering* 24: 103315.

Amer M, Chen Z, Du Y, Mashrah WAH, Zhang W (2023) Experimental and numerical investigations on cyclic performance of L-shaped-CFT column frame-buckling restrained and unrestrained steel plate shear walls with partial double-side/four corner connections. *Journal of Building Engineering* 78: 107568.

ANSYS (2016) *ANSYS User's Manual Revision 16.0*. ANSYS, Inc.

Du Y, Zhang Y, Chen Z, Dong S, Deng X-f, Qian K (2021) Seismic behavior of CFRP confined rectangular CFST columns using high-strength materials: Numerical analysis and restoring force model. *Structures* 34: 4237–4253.

Güneyisi EM, Nour AI (2019) Axial compression capacity of circular CFST columns transversely strengthened by FRP. *Engineering Structures* 191: 417–431.

Kent DC, Park R (1971) Flexural Members with Confined Concrete. *Journal of the Structural Division* 97(7): 1969–1990.

Ren FM, Lai CL, Guo JY, Chen GM, Tao Y, Xie P (2022) Concrete-Filled Multicellular Steel-Tube Shear Walls with FRP Tubes Embedded in CFST: Concept and Seismic Performance. *Journal of Composites for Construction* 26(6): 04022072.

Shaaban IG, Said M (2018) Finite element modeling of exterior beam-column joints strengthened by ferrocement under cyclic loading. *Case Studies in Construction Materials* 8: 333–346.

Shen Q, Wu T, Wang J, Wang F, Zhu W, Peng X (2024) Dynamic response and design evaluation of circular CFT columns with ring-shaped voids under transverse impact. *Composite Structures* 328: 117743.

Teng JG, Hu YM, Yu T (2013) Stress–strain model for concrete in FRP-confined steel tubular columns. *Engineering Structures* 49: 156–167.

Teng JG, Yu T, Fernando D (2012) Strengthening of steel structures with fiber-reinforced polymer composites. *Journal of Constructional Steel Research* 78: 131–143.

Xiao Y (2004) Applications of FRP Composites in Concrete Columns. *Advances in Structural Engineering* 7(4): 335–343.

Yu T, Hu YM, Teng JG (2016) Cyclic lateral response of FRP-confined circular concrete-filled steel tubular columns. *Journal of Constructional Steel Research* 124: 12–22.

Zeng J-J, Zheng Y-W, Liu F, Guo Y-C, Hou C (2021) Behavior of FRP Ring-Confined CFST columns under axial compression. *Composite Structures* 257: 113166.